2018

# Analysis of the Red and Green Optical Absorption Spectrum of Gas Phase Ammonia

Nikolai F. Zobov

Phillip A. Coles

Roman I. Ovsyannikov

Aleksandra A. Kyuberis

Robert J. Hargreaves

*See next page for additional authors*



## Original Publication Citation

Zobov, N. F., Coles, P. A., Ovsyannikov, R. I., Kyuberis, A. A., Hargreaves, R. J., Bernath, P. F., Tennyson, J., Yurchenko, S. N., & Polyansky, O. L. (2018). Analysis of the red and green optical absorption spectrum of gas phase ammonia. *Journal of Quantitative Spectroscopy & Radiative Transfer*, *209*, 224-231. https://doi.org/10.1016/j.jcprt.2018.02.001

Journal of Quantitative Spectroscopy & Radiative Transfer 209 (2018) 224–231

Contents lists available at ScienceDirect

Journal of Quantitative Spectroscopy & Radiative Transfer

journal homepage: www.elsevier.com/locate/jqsrt

# Analysis of the red and green optical absorption spectrum of gas phase ammonia

Nikolai F. Zobov[a], Phillip A Coles[b], Roman I. Ovsyannikov[a], Aleksandra A. Kyuberis[a], Robert J. Hargreaves[c], Peter F. Bernath[d], Jonathan Tennyson[b,*], Sergei N. Yurchenko[b], Oleg L. Polyansky[b,a]

[a] Institute of Applied Physics, Russian Academy of Science, Ulyanov Street 46, Nizhny Novgorod 603950, Russia
[b] Department of Physics and Astronomy, University College London, Gower Street, London WC1E 6BT, UK
[c] Atmospheric, Oceanic & Planetary Physics, University of Oxford, Clarendon Laboratory, Parks Road, Oxford OX1 3PU, UK
[d] Department of Chemistry and Biochemistry, Old Dominion University, Norfolk, VA 23527, USA

ARTICLE INFO

*Article history:*
Received 24 October 2017
Revised 1 February 2018
Accepted 1 February 2018
Available online 9 February 2018

*Keywords:*
Ammonia
Vibration-rotation
Visible
Line list

ABSTRACT

Room temperature $NH_3$ absorption spectra recorded at the Kitt Peak National Solar Observatory in 1980 are analyzed. The spectra cover two regions in the visible: 15,200 – 15,700 $cm^{-1}$ and 17,950 – 18,250 $cm^{-1}$. These high overtone rotation-vibration spectra are analyzed using both combination differences and variational line lists. Two variational line lists were computed using the TROVE nuclear motion program: one is based on an *ab initio* potential energy surface (PES) while the other used a semi-empirical PES. *Ab initio* dipole moment surfaces are used in both cases. 95 energy levels with $J = 1 - 7$ are determined from analysis of the experimental spectrum in the $5\nu_{NH}$ (red) region and 46 for $6\nu_{NH}$ (green) region. These levels span four vibrational bands in each of the two regions, associated with stretching overtones.



## 1. Introduction

There are a number of reasons why one might attempt to analyse the high resolution optical ro-vibrational spectrum of ammonia. Firstly, the spectrum of ammonia is a textbook example of high resolution molecular spectroscopy. However, for almost 70 years, the vibration-rotation spectrum of $^{14}NH_3$ was only studied in detail at wavelengths longer than 2 μm; these spectra are assembled in comprehensive high resolution molecular spectroscopic databases such as the 2008 edition of HITRAN [1]. Only relatively recently and rather gradually has the absorption spectrum of $NH_3$ been successfully analyzed in the near infrared region [2–8]; some of these data are included in the recent, 2016, release of HITRAN [9]. The spectrum of ammonia at visible wavelengths remains poorly characterized and, at best, only partially analyzed. A full review of high resolution, vibration-rotation studies of $^{14}NH_3$ was recently provided by Al Derzi et al. [10] as part of their MARVEL (measured active rotation-vibration energy levels) study of the molecule.

Secondly, there is renewed interest in the spectrum of ammonia caused by attempts to analyze spectra of brown dwarfs [11], and in particular the fact that the coldest of these object, Y-dwarfs, should be characterized by strong ammonia features [12,13], but possibly are not. Nonetheless, detailed ammonia spectra have been assigned in brown dwarfs [11]. The discovery of the exoplanets, and especially the use of the transit method to observe molecular spectra [14], has led to discussions on the presence of ammonia in these objects too [15,16]. Water and methane are essential to the characterization of exoplanetary spectra. However, ammonia may be a "mind-marker" as ammonia is the most-manufactured molecule on Earth and is also a major byproduct of intensive agriculture, and hence a possible sign of intelligent life. Ammonia is among a number of molecules being actively discussed as a possible bio-marker [17,18]. Ammonia has recently been detected in the atmosphere of a hot Jupiter exoplanet [19].

Thirdly, the umbrella motion in $NH_3$ is a classic example of a molecule undergoing a large amplitude motion. The effect of this motion on the energy levels in the system has been the subject of recent careful analysis [20]. However, the corresponding energy levels for higher states remain unknown. The spectrum of ammonia remains hard to calculate accurately and to analyse [21] due to

* Corresponding author.
*E-mail addresses:* j.tennyson@ucl.ac.uk (J. Tennyson), o.polyansky@ucl.ac.uk (O.L. Polyansky).

https://doi.org/10.1016/j.jqsrt.2018.02.001

**Table 1**
Calculated vibrational band centers and band intensities using our two different PESs and our most reliable DMS. Units of intensity are $cm^{-1}/(molecules\ cm^{-2})$ and units of frequency are $cm^{-1}$.

| Symmetry | $(\upsilon_1\upsilon_2\upsilon_3L_3\upsilon_4L_4$ s/a) | $\nu_0^{ai}$ | $I_0^{ai}$ | $\nu_0^{ref}$ | $I_0^{ref}$ |
|---|---|---|---|---|---|
| $A_1'$ | 5 0 0 0 0 0 s | 15,463.3924 | $2.412 \times 10^{-22}$ | 15,445.9471 | $2.686 \times 10^{-22}$ |
| $A_2''$ | 5 0 0 0 0 0 a | 15,461.3950 | $1.039 \times 10^{-22}$ | 15,447.2406 | $2.512 \times 10^{-22}$ |
| $E'$ | 4 0 1 1 0 0 a | 15,463.5532 | $6.454 \times 10^{-23}$ | 15,445.5068 | $6.731 \times 10^{-23}$ |
| $E''$ | 4 0 1 1 0 0 s | 15,462.4164 | $7.176 \times 10^{-23}$ | 15,446.9127 | $5.780 \times 10^{-23}$ |
| $A_1'$ | 6 0 0 0 0 0 s | 18,131.8294 | $8.271 \times 10^{-23}$ | 18,106.5124 | $6.338 \times 10^{-23}$ |
| $A_2''$ | 6 0 0 0 0 0 a | 18,144.9957 | $6.855 \times 10^{-23}$ | 18,118.3103 | $4.262 \times 10^{-23}$ |
| $E'$ | 5 0 1 1 0 0 a | 18,132.3858 | $3.907 \times 10^{-23}$ | 18,106.7462 | $1.568 \times 10^{-23}$ |
| $E''$ | 5 0 1 1 0 0 s | 18,145.0979 | $3.540 \times 10^{-23}$ | 18,118.3656 | $9.478 \times 10^{-24}$ |

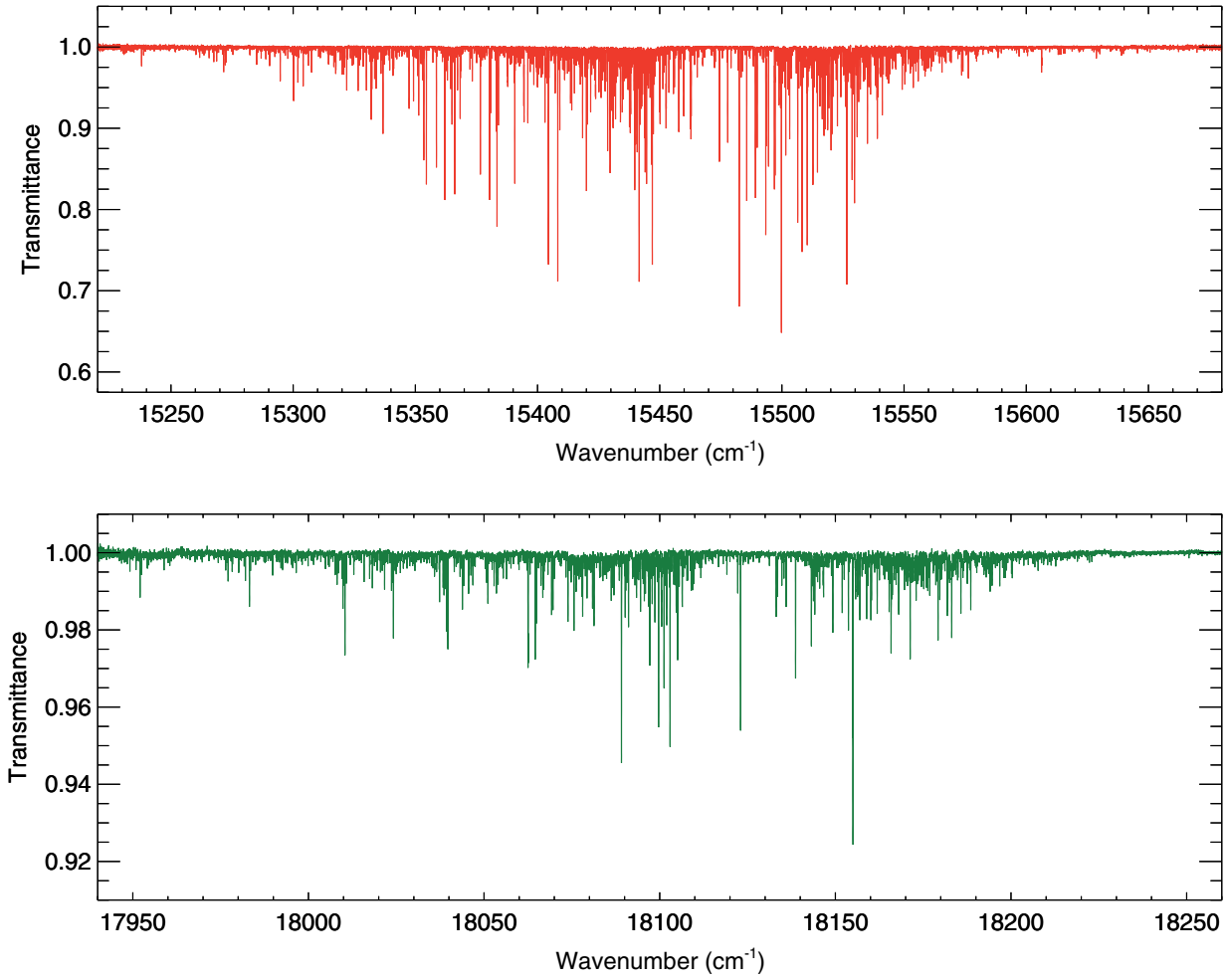


**Fig. 1.** Overview transmission spectra calculated from the Kitt Peak Fourier transform spectra 800406R0.007 (upper) and 800407R0.001 (lower).

this unusual umbrella motion. This is especially true for states of high vibrational excitation such as those found in its visible spectrum.

Finally, transitions at visible wavelengths provide a pathway to the study of the spectrum of ammonia up to and beyond dissociation. For the isoelectronic water molecule, the use of multiple-resonance visible-wavelength spectra has provided a direct route to dissociation [22] and beyond [23].

In fact, visible wavelength spectra have been available for some time. Ammonia lines in this region were observed at Kitt Peak in 1980, but remained unanalyzed; see next section. This work was directly followed by dye laser experiments by Kuga et al. [24] and microwave-detected microwave-optical double resonance studies by Coy and Lehmann [25–27]. About 1000 ammonia transitions in the 15,260 – 15,590 $cm^{-1}$ region were measured by Kugu et al. [24] using Stark modulation with 193 of them being given rotation assignments. Coy and Lehmann [25] recorded visible ammonia spectra around 15,450 and 18,110 $cm^{-1}$ with both photoacoustic absorption and microwave-optical double resonance spectra techniques. Again rotational assignments, only, were given for 318 and 105 lines respectively in the two regions. These partial (rotational) assignments do not supply information on the upper vibrational state. It is only very recently, with the advent of high quality *ab initio* studies, that vibrational assignments have begun to emerge *e.g.* [28].

This paper is organized as follows. Section 2 provides a description of the Kitt Peak observation of ammonia in the optical region. Section 3 presents our analysis of this spectrum and Section 4 compares the results with those of previous studies. Conclusions are made in Section 5.

**Table 2**
Observed ammonia energy levels, in $cm^{-1}$, in the $5\nu_{NH}$ region: also given are the calculated values with both the *ab initio* (ai) and refined (ref) PESs, the observed minus calculated (o-c) residues and error in the combination difference (CD).

| J | K | calc. ai | obs. | o-c | CD | calc.ref | o-c |
|---|---|---|---|---|---|---|---|
| 5 0 0 0 0 0 $A_1'$ s | | | | | | | |
| 1 | 1 | 15,478.3353 | 15,466.5198 | −11.82 | 0.0015 | 15,461.5691 | 4.95 |
| 3 | 0 | 15,573.5648 | 15,561.9812 | −11.58 | −0.0012 | 15,556.3977 | 5.58 |
| 3 | 3 | 15,545.9218 | 15,533.4884 | −12.43 | −0.0008 | 15,528.5446 | 4.94 |
| 4 | 2 | 15,633.3132 | 15,621.4179 | −11.90 | −0.0003 | | |
| 4 | 3 | 15,618.7333 | 15,605.8568 | −12.88 | 0.0006 | 15,601.5825 | 4.27 |
| 5 | 3 | 15,710.0286 | 15,697.4938 | −12.53 | 0.0030 | 15,692.9553 | 4.54 |
| 6 | 3 | 15,818.4972 | 15,806.3031 | −12.19 | 0.0062 | 15,801.6672 | 4.63 |
| 7 | 6 | 15,865.8936 | 15,853.4710 | −12.42 | −0.0001 | 15,848.2242 | 5.25 |
| 4 0 1 1 0 0 E′ s | | | | | | | |
| 1 | 0 | 15,481.8660 | 15,469.9316 | −11.93 | −0.0012 | 15,463.9325 | 6.00 |
| 1 | 1 | 15,478.9618 | 15,466.4888 | −12.47 | −0.0012 | 15,461.0864 | 5.40 |
| 2 | 0 | 15,518.6451 | 15,506.0918 | −12.55 | 0.0004 | | |
| 2 | 1 | 15,514.5842 | 15,502.4293 | −12.15 | −0.0003 | 15,496.5855 | 5.84 |
| 2 | 1 | 15,516.3664 | 15,502.9113 | −13.46 | 0.0047 | 15,496.6968 | 6.21 |
| 2 | 2 | 15,505.9747 | 15,494.0029 | −11.97 | 0.0006 | 15,488.2554 | 5.75 |
| 2 | 2 | 15,506.1888 | 15,494.1377 | −12.05 | | | |
| 3 | 0 | 15,574.1047 | 15,562.1522 | −11.95 | −0.0008 | 15,555.8965 | 6.26 |
| 3 | 1 | 15,572.2321 | 15,563.0706 | −9.16 | −0.0046 | 15,551.0073 | 12.06 |
| 3 | 1 | 15,572.4357 | 15,560.8323 | −11.60 | | 15,554.3331 | 6.50 |
| 3 | 2 | 15,560.6454 | 15,548.7502 | −11.90 | −0.0015 | 15,542.8740 | 5.88 |
| 3 | 2 | 15,561.1995 | 15,549.4616 | −11.74 | −0.0019 | 15,543.0635 | 6.40 |
| 3 | 3 | 15,544.8852 | 15,533.9636 | −10.92 | 0.0000 | 15,527.7201 | 6.24 |
| 3 | 3 | 15,546.0406 | 15,533.9637 | −12.08 | 0.0000 | 15,527.9310 | 6.03 |
| 4 | 1 | 15,640.8673 | 15,627.6109 | −13.26 | −0.0001 | 15,623.1372 | 4.47 |
| 4 | 2 | 15,634.6141 | 15,622.2864 | −12.33 | 0.0003 | 15,615.6958 | 6.59 |
| 4 | 2 | 15,634.7014 | 15,623.1377 | −11.56 | −0.0007 | 15,616.7113 | 6.43 |
| 4 | 3 | 15,619.3581 | 15,607.5985 | −11.76 | −0.0006 | 15,601.0887 | 6.51 |
| 4 | 3 | 15,619.1095 | 15,606.9873 | −12.12 | 0.0013 | 15,601.1311 | 5.86 |
| 4 | 4 | 15,597.5857 | 15,585.6611 | −11.92 | 0.0006 | 15,579.9239 | 5.74 |
| 4 | 4 | 15597.8406 | 15,588.6857 | −9.15 | −0.0040 | 15,575.7678 | 12.92 |
| 5 | 0 | 15,740.7703 | 15,727.8952 | −12.88 | 0.0001 | 15,722.4298 | 5.47 |
| 5 | 1 | 15,739.9982 | 15,726.3129 | −13.69 | | 15,722.0249 | 4.29 |
| 5 | 2 | 15,723.6043 | 15,709.8891 | −13.72 | 0.0017 | 15,705.7193 | 4.17 |
| 5 | 3 | 15,709.8405 | 15,697.9178 | −11.92 | 0.0059 | 15,692.1836 | 5.73 |
| 5 | 4 | 15,689.1987 | 15,677.2516 | −11.95 | −0.0013 | | |
| 5 | 4 | 15,689.5117 | 15,678.0245 | −11.49 | 0.0002 | | |
| 5 | 5 | 15,661.6004 | 15,649.7260 | −11.87 | −0.0015 | 15,644.0356 | 5.69 |
| 5 | 5 | 15,661.8454 | 15,649.7205 | −12.12 | −0.0044 | | |
| 6 | 1 | 15,839.8586 | 15,825.9434 | −13.92 | 0.0028 | 15,822.1480 | 3.80 |
| 6 | 2 | 15,836.1023 | 15,823.5558 | −12.55 | −0.0002 | 15,818.3883 | 5.17 |
| 6 | 4 | 15,798.8243 | 15,783.9469 | −14.88 | 0.0074 | | |
| 6 | 5 | 15,771.3477 | 15,759.1135 | −12.23 | −0.0001 | 15,753.7410 | 5.37 |
| 6 | 5 | 15,771.4733 | 15,759.2062 | −12.27 | 0.0006 | 15,753.9483 | 5.26 |
| 6 | 6 | 15,737.6585 | 15,725.3892 | −12.27 | 0.0025 | 15,719.1815 | 6.21 |
| 6 | 6 | 15,737.9054 | 15,725.6116 | −12.29 | −0.0011 | 15,720.1091 | 5.50 |
| 7 | 4 | 15,926.0570 | 15,913.8181 | −12.24 | −0.0044 | 15,908.4322 | 5.39 |
| 7 | 5 | 15,899.3692 | 15,886.8414 | −12.53 | −0.0036 | 15,882.3011 | 4.54 |
| 7 | 7 | 15,825.4482 | 15,813.2774 | −12.17 | 0.0093 | 15,808.0481 | 5.23 |
| 7 | 7 | 15,826.4303 | 15,813.2773 | −13.15 | 0.0093 | | |
| 5 0 0 0 0 0 $A_2''$ a | | | | | | | |
| 2 | 0 | 15,517.0588 | 15,502.4293 | −14.63 | −0.0003 | 15,502.2533 | 0.18 |
| 3 | 3 | 15,544.4086 | 15,530.4653 | −13.94 | 0.0013 | 15,529.8940 | 0.57 |
| 4 | 0 | 15,646.1915 | 15,633.7890 | −12.40 | 0.0006 | 15,631.2144 | 2.57 |
| 4 | 3 | 15,617.4028 | 15,601.4186 | −15.98 | −0.0006 | 15,602.8596 | -1.44 |
| 5 | 3 | 15,708.2297 | 15,694.0690 | −14.16 | 0.0019 | 15,693.6011 | 0.47 |
| 6 | 3 | 15,817.6447 | 15,804.6638 | −12.98 | 0.0000 | 15,801.5010 | 3.16 |
| 6 | 6 | 15736.4654 | 15,723.6854 | −12.78 | 0.0084 | | |
| 7 | 3 | 15,943.1415 | 15,928.5263 | −14.62 | −0.0046 | 15,928.3130 | 0.21 |
| 4 0 1 1 0 0 E′′ a | | | | | | | |
| 1 | 0 | 15,480.7408 | 15,466.9949 | −13.75 | 0.0053 | 15,465.2181 | 1.78 |
| 1 | 1 | 15,477.3769 | 15,463.4543 | −13.92 | 0.0052 | 15,461.8168 | 1.64 |
| 2 | 0 | 15,517.4444 | 15,503.8631 | −13.58 | 0.0002 | 15,501.6522 | 2.21 |
| 2 | 1 | 15,515.2109 | 15,500.1851 | −15.03 | | | |
| 2 | 1 | 15,515.0942 | 15,501.2087 | −13.89 | −0.0009 | 15,496.6968 | 4.51 |
| 2 | 2 | 15,504.9696 | 15,491.3928 | −13.58 | 0.0022 | 15,489.3425 | 2.05 |
| 2 | 2 | 15,505.2649 | 15,491.3928 | −13.87 | 0.0008 | 15,485.4882 | 5.90 |
| 3 | 0 | 15,572.6798 | 15,560.0324 | −12.65 | 0.0000 | 15,556.9058 | 3.13 |
| 3 | 1 | 15,567.3094 | 15,553.8064 | −13.50 | −0.0007 | 15,551.0073 | 2.80 |
| 3 | 2 | 15,559.7436 | 15,546.4812 | −13.84 | 0.0003 | 15,543.0635 | 3.42 |
| 3 | 2 | 15,559.9225 | 15,546.5713 | −13.35 | 0.0009 | | |
| 3 | 2 | 15,560.3182 | 15,546.4812 | −13.84 | 0.0003 | 15,540.7744 | 5.71 |
| 3 | 3 | 15,544.7225 | 15,531.1917 | −13.53 | −0.0007 | 15,529.1457 | 2.05 |
| 4 | 0 | 15,646.5022 | 15,631.1398 | −15.36 | 0.0016 | 15,630.9364 | 0.20 |

(*continued on next page*)

**Table 2** (*continued*)

| J | K | calc. ai | obs. | o-c | CD | calc.ref | o-c |
|---|---|---|---|---|---|---|---|
| 4 | 1 | 15,639.2451 | 15,625.0227 | −14.22 | −0.0022 | 15,624.0756 | 0.95 |
| 4 | 1 | 15,645.3214 | 15,630.2131 | −15.11 | 0.0014 | | |
| 4 | 2 | 15,631.8889 | 15,618.6802 | −13.21 | 0.0010 | 15,615.6958 | 2.98 |
| 4 | 2 | 15,633.0966 | 15,619.2053 | −13.89 | 0.0025 | | |
| 4 | 3 | 15,617.7110 | 15,603.9518 | −13.76 | −0.0011 | 15,601.1311 | 2.82 |
| 4 | 3 | 15,617.7948 | 15,607.7478 | −10.05 | 0.0062 | 15,601.9253 | 5.82 |
| 4 | 4 | 15,596.4500 | 15,583.5915 | −12.86 | −0.0010 | 15,581.0460 | 2.55 |
| 5 | 0 | 15,738.9750 | 15,724.3296 | −14.65 | −0.0096 | 15,722.7391 | 1.59 |
| 5 | 1 | 15,729.6859 | 15,717.0764 | −12.61 | 0.0017 | 15,721.2442 | -4.17 |
| 5 | 3 | 15,708.5130 | 15,696.0748 | −12.44 | −0.0017 | 15,693.0882 | 2.99 |
| 5 | 3 | 15,708.9455 | 15,694.7899 | −14.16 | 0.0001 | 15,692.4417 | 2.35 |
| 5 | 4 | 15,687.7743 | 15,674.3339 | −13.44 | 0.0004 | 15,672.2831 | 2.05 |
| 5 | 4 | 15,687.8374 | 15,674.3682 | −13.47 | −0.0046 | | |
| 5 | 5 | 15,660.5921 | 15,646.6242 | −13.97 | −0.0043 | 15,644.0356 | 2.59 |
| 5 | 5 | 15,660.6026 | 15,646.4553 | −14.15 | −0.0021 | 15,644.2257 | 2.23 |
| 6 | 1 | 15,850.0131 | 15,836.8953 | −13.12 | 0.0026 | 15,830.1096 | 6.79 |
| 6 | 2 | 15,829.5421 | 15,815.1499 | −14.39 | −0.0019 | 15,813.9548 | 1.20 |
| 6 | 4 | 15,796.8984 | 15,782.4646 | −14.43 | 0.0025 | 15,780.8148 | 1.65 |
| 6 | 5 | 15,769.8239 | 15,756.1173 | −13.71 | −0.0045 | 15,753.9951 | 2.12 |
| 6 | 5 | 15,770.0171 | 15,759.2062 | −10.81 | 0.0006 | 15,753.7410 | 5.47 |
| 6 | 6 | 15,737.0255 | 15,721.9501 | −15.08 | −0.0047 | 15,720.1091 | 1.84 |
| 7 | 1 | 15,964.6886 | 15,950.3221 | −14.37 | 0.0052 | 15,963.2702 | −12.95 |
| 7 | 2 | 15,962.1867 | 15,947.3398 | −14.85 | −0.0041 | 15,946.6881 | 0.65 |
| 7 | 4 | 15,924.0102 | 15,910.2483 | −13.76 | −0.0030 | 15,903.9761 | 6.27 |
| 7 | 6 | 15,864.3182 | 15,851.2255 | −13.09 | −0.0007 | 15,849.0868 | 2.14 |
| 7 | 7 | 15,824.9631 | 15,810.9749 | −13.99 | −0.0047 | 15,808.7132 | 2.26 |

## 2. Experimental observation of ammonia spectra

The two ammonia spectra were recorded with the McMath-Pierce Fourier transform spectrometer (FTS) of the National Solar Observatory at Kitt Peak. The red spectrum centered at 647 nm was recorded on April 6, 1980 by C. de Bergh, R. Hubbard and J. Brault (800406R0.007 in the archive). The ammonia sample was held in a White-type multireflection cell with a base path length of 6 m. The cell was set for 72 passes (432 m total path length) and the sample had a pressure of 7.8 Torr at room temperature (20.6 °C). The FTS used the Visible beamsplitter (fused silica with a silver coating), silicon photodiode detectors and a quartz halogen lamp as a light source. The optical bandpass was set to 15200–15700 $cm^{-1}$ with an OG570 color filter and a tilted Corion 660 nm bandpass filter. Forty scans were co-added in 5 h of integration at a resolution of 0.024 $cm^{-1}$.

The green spectrum centered at 551 nm was recorded on April 7, 1980 by C. de Bergh, J. Brault and D. Jennings (800407R0.001 in the archive) with a similar experimental arrangement. The sample had a pressure of 10.88 Torr at room temperature (21.5 °C). The optical bandpass was set to 17950–18250 $cm^{-1}$ with a tilted Corion 560 nm bandpass filter. Thirty-six scans were co-added in 4.5 h of integration at a resolution of 0.034 $cm^{-1}$.

The spectra are shown in Fig. 1; they were analyzed by creating a baseline and calculating transmission spectra. The spectra were fitted to create line lists containing the line position and an arbitrary intensity for each feature. The line positions were calibrated (using HITRAN [29]) based on water absorption lines in two lower spectral regions recorded in the same run under similar conditions, and the same calibration factor has been applied to all line lists. The line lists are given as supplementary data to this paper.

## 3. Spectral analysis

The ammonia absorption spectra were recorded at room temperature in the 15,200 – 15,700 $cm^{-1}$ and 17,950 – 18,250 $cm^{-1}$ regions. These regions are the ones with the strongest ammonia absorption; the strongest lines belong to pure stretching overtone excitations of $\nu_1$ and $\nu_3$.

At $T = 296$ K, our spectrum in the 15,000 $cm^{-1}$ region contains 1069 lines stronger than $5 \times 10^{-26}$ cm/molecule and 550 lines in the 18, 000 $cm^{-1}$ region stronger than $10^{-26}$ cm/molecule. Analysis of the spectra was based on two variational line lists. The two line lists differ in the potential energy surface (PES) employed: *ab initio* [28] and semi-empirical [30], but used the same *ab initio* dipole moment surface (DMS) [31] in both cases. The resulting differences in calculated band centers and band intensities are shown in Table 1, where we have used a DMS specifically produced to be accurate at high frequencies. Both the DMS used in the assignments, and that used to calculated band intensities will be discussed elsewhere [30]. Spectra were calculated using the variational nuclear motion program TROVE [32,33], which has been especially adapted to treat ammonia [34].

234 and 107 lines are assigned in the respective regions, mostly using the method of combination differences. The six strongest lines in 15,000 $cm^{-1}$ region were assigned by direct comparison with the variational line list on the basis of comparing theoretical and experimental frequencies and intensities. These assignment lead to determination of 95 and 46 energy levels in $5\nu_{NH}$ and $6\nu_{NH}$ regions, respectively. Our line list predicts a line about every 0.1 $cm^{-1}$, but the standard deviation of differences between observed frequencies and experimental levels is only 0.003 $cm^{-1}$ for the $5\nu_{NH}$ and 0.006 $cm^{-1}$ for the $6\nu_{NH}$ regions, which means that combination differences provides a reliable means of identifying transitions.

Table 2 presents the experimentally-derived energy levels for $\nu_{NH}$ =5 states of $^{14}NH_3$, together with their rotational quantum number $J$ and $K$ assignment. The vibrational assignments are taken from the TROVE line lists. Vibrational assignments use standard normal-mode style quantum numbers [35]. While they were informed by the quantum numbers provided by TROVE, which uses its own convention, they were largely determined by energy values and symmetry.

The difference between combination differences derived from the experimental lines of this work and the known ground states presented in the MARVEL database [10] is ususally less than 0.001 $cm^{-1}$. This practically excludes the possibility of fortuitous coincidences and confirms the various assignments. The assigned

**Table 3**
Observed ammonia energy levels, in $cm^{-1}$, in the $6\nu_{NH}$ region also given are the calculated values with both the *ab initio* (ai) and refined (ref) PESs, the observed minus calculated (o-c) residues and error in the combination difference (CD).

| *J* | *K* | calc. ai | obs. | o-c | CD | calc.ref | o-c |
|---|---|---|---|---|---|---|---|
| 6 0 0 0 0 0 $A_1'$ s | | | | | | | |
| 1 | 0 | 18,150.23 | 18,122.9443 | −27.29 | 0.0049 | 18,125.3154 | −2.37 |
| 2 | 2 | 18,174.19 | 18,148.2950 | −25.90 | 0.0002 | 18,149.5133 | −1.22 |
| 3 | 0 | 18,242.65 | 18,216.6530 | −26.00 | 0.0007 | 18,218.0140 | −1.36 |
| 3 | 2 | 18,229.49 | 18,202.5104 | −26.98 | 0.0090 | 18,205.4781 | −2.97 |
| 3 | 3 | 18,213.58 | 18,187.1485 | −26.43 | 0.0090 | 18,189.0091 | −1.86 |
| 3 | 3 | 18,214.51 | 18,185.2380 | −29.28 | 0.0100 | 18,189.3351 | −4.10 |
| 4 | 3 | 18,287.87 | 18,262.2755 | −25.59 | 0.0050 | | |
| 6 | 6 | 18,407.08 | 18,382.0507 | −25.03 | 0.0097 | 18,381.8783 | 0.17 |
| 5 0 1 1 0 0 E′ s | | | | | | | |
| 2 | 1 | 18,184.35 | 18,158.5039 | −25.85 | 0.0002 | 18,159.1471 | −0.64 |
| 3 | 1 | 18,240.38 | 18,216.3554 | −24.03 | 0.0102 | | |
| 3 | 2 | 18,229.36 | 18,203.8817 | −25.49 | 0.0080 | 18,204.9315 | −1.05 |
| 3 | 3 | 18,214.47 | 18,190.2721 | −24.21 | 0.0021 | 18,188.5726 | 1.70 |
| 4 | 1 | 18,308.95 | 18,281.0925 | −27.86 | 0.0016 | 18,284.2971 | −3.20 |
| 4 | 4 | 18,266.42 | 18,239.5275 | −26.90 | 0.0065 | 18,240.9899 | −1.46 |
| 5 | 4 | 18,358.66 | 18,336.4739 | −22.19 | 0.0010 | 18,333.4767 | 3.00 |
| 5 | 5 | 18,331.34 | 18,308.2101 | −23.13 | 0.0061 | | |
| 6 | 5 | 18,441.80 | 18,419.7385 | −22.07 | 0.0078 | 18,416.3563 | 3.38 |
| 6 | 6 | 18,407.70 | 18,381.9761 | −25.73 | 0.0045 | 18,381.1558 | 0.82 |
| 6 0 0 0 0 0 $A_2''$ a | | | | | | | |
| 2 | 0 | 18,200.04 | 18,174.5032 | −25.54 | 0.0074 | 18,172.9909 | 1.51 |
| 3 | 2 | 18,243.85 | 18,216.6809 | −27.18 | 0.0021 | 18,218.1875 | −1.50 |
| 3 | 3 | 18,226.94 | 18,198.4299 | −28.51 | 0.0064 | 18,200.5128 | −2.08 |
| 4 | 0 | 18,329.36 | 18, 303.4852 | −25.88 | 0.0075 | 18,303.4155 | 0.07 |
| 5 0 1 1 0 0 E′′ a | | | | | | | |
| 1 | 1 | 18,140.65 | 18,115.9028 | −24.76 | 0.0078 | 18,116.3720 | −0.47 |
| 2 | 0 | 18,180.53 | 18,152.2634 | −28.27 | 0.0109 | 18,156.2881 | −4.02 |
| 2 | 0 | 18,200.14 | 18,179.6675 | −20.48 | 0.0061 | | |
| 2 | 1 | 18,179.29 | 18,157.5306 | −21.76 | 0.0024 | | |
| 2 | 2 | 18,187.98 | 18,164.4116 | −23.57 | 0.0011 | | |
| 3 | 0 | 18,255.15 | 18,230.2401 | −24.91 | 0.0074 | 18,229.5317 | 0.71 |
| 3 | 1 | 18,234.98 | 18,209.6301 | −25.35 | 0.0033 | 18,209.6730 | −0.04 |
| 3 | 2 | 18,242.93 | 18,215.8869 | −27.05 | 0.0106 | | |
| 3 | 2 | 18,243.76 | 18,216.7658 | −27.00 | 0.0034 | | |
| 3 | 3 | 18,226.75 | 18,200.4632 | −26.29 | 0.0099 | | |
| 4 | 0 | 18,329.30 | 18,300.2546 | −29.05 | 0.0053 | | |
| 4 | 1 | 18,311.25 | 18,286.2913 | −24.97 | 0.0084 | 18,286.6713 | −0.38 |
| 4 | 2 | 18,301.21 | 18,275.2713 | −25.95 | 0.0040 | 18,274.3152 | 0.96 |
| 4 | 2 | 18,317.32 | 18,290.4768 | −26.85 | 0.0010 | 18,293.0889 | −2.61 |
| 4 | 3 | 18,302.79 | 18,277.2233 | −25.58 | 0.0061 | | |
| 4 | 4 | 18,259.61 | 18,237.3512 | −22.26 | 0.0003 | 18,238.2487 | −0.90 |
| 4 | 4 | 18,259.96 | 18,232.3751 | −27.59 | 0.0126 | | |
| 5 | 1 | 18,416.37 | 18,393.2933 | −23.08 | 0.0083 | | |
| 5 | 4 | 18,352.29 | 18,322.8273 | −29.47 | 0.0020 | 18,330.1106 | −7.28 |
| 5 | 5 | 18,324.25 | 18,302.6365 | −21.62 | 0.0117 | 18,303.0127 | −0.38 |
| 5 | 5 | 18,344.33 | 18,316.0527 | −28.28 | 0.0027 | 18,307.5629 | 8.49 |
| 6 | 4 | 18,481.50 | 18,450.9003 | −30.61 | 0.0075 | | |
| 6 | 6 | 18,400.89 | 18,373.0528 | −27.84 | 0.0100 | 18,380.3334 | −7.28 |
| 6 | 6 | 18,421.47 | 18,394.4531 | −27.02 | 0.0104 | | |

lines confirmed by combination differences and the corresponding experimentally-derived energy levels opens the way to assigning further lines without confirmation via combination differences. The observed minus calculated residuals given in the Tables 2 and 3 show that the discrepancy between calculated and experimentally derived levels is large but stable. This information can be used for assignment of the higher *J* and *K* lines in the future using the method of branches [36].

## 4. Comparison with previous work

Both Kuga et al. [24] and Coy and Lehmann [25–27] measured ammonia spectra at visible wavelengths. However only Coy and Lehmann published some of their actual line data and we compare with these below. In both cases the two sets of experimental wavenumbers are in good agreement. Coy and Lehmann give rotational assignments but did not attempt vibrational assignments. Our study gives full assignments which were obtained, as described above, independent of previously published results.

Table 4 compares the 42 lines presented by Coy and Lehmann [25] with our results. Our assignments suggest that Coy and Lehmann's spectra probed several upper vibrational states. However, there is good agreement between our rotational assignments and theirs: our assignments agree for 35 out of the 42 lines partially assigned by Coy and Lehmann. We have not assigned most of the other matching lines.

Table 5 compares our results with those of Coy and Lehmann [25] for the 18,000 $cm^{-1}$ region. The agreement between the assignments is less good with our work only confirming 7 of the 14 rotational assignments given by Coy and Lehmann. For these assigned lines we are also able to provide vibrational assignments.

## 5. Conclusion

We have analyzed the room-temperture absorption spectrum of ammonia in red (15,000 $cm^{-1}$) and green (18,000 $cm^{-1}$) spectral regions recorded using a long pathlength FT spectrometer. Assignment of strong lines on these two regions is made up to $J = 7$.

**Table 4**
Comparison of this work with the results of Coy and Lehmann [25] for the 15 000 $cm^{-1}$ region. Intensities, *I*, are absolute for Coy and Lehmann but are only relative (arbitrary units) for this work. $\Delta\tilde{\nu}$ is the wavenumber difference given as previous minus this work.

| Coy and Lehmann | | | This work | | | Agree? | $\Delta\tilde{\nu}/cm^{-1}$ |
|---|---|---|---|---|---|---|---|
| $\tilde{\nu}(cm^{-1})$ | $I(cm^{-1}$/km-atm) | assignment | $\tilde{\nu}(cm^{-1})$ | $I$ | assignment | | |
| 15,514.509 | 2.8 | rR 30s | 15,514.50598 | 0.165 | rR 30s 5 0 0 0 0 0 $A_2''$ a | yes | 0.003 |
| 15,512.652 | | rR 43s | 15,512.64820 | 0.192 | rR 43s 4 0 1 1 0 0 E′ s | yes | 0.004 |
| 15,512.502 | 3.53 | qR 32s | 15,512.49360 | 0.061 | | no | 0.008 |
| 15,510.319 | 6.91 | rQ 44s | 15,510.31726 | 0.276 | rR 44s 4 0 1 1 0 0 E′ s | yes | 0.002 |
| 15,508.332 | | qR 30s | 15,508.32790 | 0.145 | rR 30s 4 0 1 1 0 0 E′ s | yes | 0.004 |
| 15,508.203 | 5.49 | rQ 43a | 15,508.20078 | 0.292 | rR 43a 4 0 1 1 0 0 E′′ a | yes | 0.002 |
| 15,506.418 | 3.53 | rR 44a | 15,506.41581 | 0.245 | rR 44a 4 0 1 1 0 0 E′′ a | yes | 0.002 |
| 15,501.526 | 1.56 | qR 20a | 15,501.52301 | 0.155 | qR 20a 5 0 0 0 0 0 $A_1'$ s | yes | 0.003 |
| 15,499.758 | 6.43 | rR 33s | 15,499.75429 | 0.422 | rR 33s 4 0 1 1 0 0 E′ s | yes | 0.004 |
| 15,497.14 | | rR 33a | 15,497.13562 | 0.176 | | no | 0.004 |
| 15,496.89 | 5.60 | rR 33a | 15,496.88853 | 0.195 | rR 33a 4 0 1 1 0 0 E′′ a | yes | 0.001 |
| 15,494.49 | 1.94 | rR 33a | 15,494.48822 | 0.164 | | no | 0.002 |
| 15,493.48 | | rR 21s | 15,493.47776 | 0.134 | rR 21s 4 0 1 1 0 0 E′ s | yes | 0.000 |
| 15,493.351 | 4.83 | rR 20a | 15,493.34820 | 0.275 | rR 20a 4 0 1 1 0 0 E′′ a | yes | 0.003 |
| 15,489.819 | 1.73 | rR 21a | 15,489.81697 | 0.130 | rR 21a 4 0 1 1 0 0 E′′ a | yes | 0.002 |
| 15,489.127 | 2.98 | rR 22s | 15,489.12250 | 0.210 | rR 22s 4 0 1 1 0 0 E′ s | yes | 0.005 |
| 15,485.56 | 2.58 | rR 22a | 15,485.55930 | 0.214 | rR 22a 4 0 1 1 0 0 E′′ a | yes | 0.001 |
| 15,482.497 | 4.96 | (q,r)R 10s | 15,482.49427 | 0.389 | rR 10s 4 0 1 1 0 0 E′ s | yes | 0.003 |
| 15,477.789 | 2.03 | rR 11s | 15,477.78477 | 0.130 | rR 11s 4 0 1 1 0 0 E′ s | yes | 0.004 |
| 15,474.386 | 2.09 | rR 11a | 15,474.38434 | 0.158 | rR 11a 4 0 1 1 0 0 E′′ a | yes | 0.002 |
| 15,462.75 | | rR 00a | 15,462.74593 | 0.122 | | no | 0.004 |
| 15,462.618 | 3.96 | rR 00a | 15,462.61582 | 0.114 | rR 00a 4 1 1 1 0 0 E′′ a | yes | 0.002 |
| 15,457.765 | 1.4 | pQ 43s | 15,457.76154 | 0.113 | pQ 43s 4 0 1 1 0 0 E′ s | yes | 0.003 |
| 15,452.624 | | pQ 32a | 15,452.62541 | 0.045 | | no | −0.001 |
| 15,452.55 | 2.8 | pQ 43a | 15,452.54721 | 0.093 | pQ 43a 4 0 1 1 0 0 E′′ a | yes | 0.003 |
| 15,450.11 | | unassigned | 15,450.10805 | 0.094 | qQ 21s 4 0 1 1 0 0 E′ s | new | 0.002 |
| 15,449.989 | 2.86 | pQ 11a | 15,449.98649 | 0.083 | pQ 11a 4 1 1 1 0 0 E′′ a | yes | 0.003 |
| 15,446.926 | 5.43 | rQ 10s | 15,446.92161 | 0.318 | rQ 10s 4 0 1 1 0 0 E′ s | yes | 0.004 |
| 15,441.553 | 4.02 | rQ 20a | 15,441.54944 | 0.348 | rQ 30s 4 0 1 1 0 0 $A_1'$ s | no | 0.004 |
| 15,429.657 | | rQ 40a | 15,429.65465 | 0.169 | pQ 51a 4 0 1 1 0 0 $A_2''$ a | no | 0.002 |
| 15,429.504 | 4.69 | rQ 32s | 15,429.49786 | 0.107 | rQ 32s 4 0 1 1 0 0 E′ s | yes | 0.006 |
| | and | qQ 53s | 15,429.49786 | 0.107 | qQ 53s 5 0 0 0 0 0 $A_2''$ a | yes | |
| 15,408.235 | 4.25 | pP 33s | 15,408.23118 | 0.336 | pP 33s 4 0 1 1 0 0 E′ s | yes | 0.004 |
| 15,404.406 | 4.52 | pP 33a | 15,404.40490 | 0.310 | pP 33a 4 0 1 1 0 0 E′′ a | yes | 0.001 |
| 15,403.129 | | rP 20a | 15,403.12551 | 0.029 | | no | 0.003 |
| 15,402.996 | 2.24 | rP 20a | 15,402.99117 | 0.096 | rP 20a 4 0 1 1 0 0 E′′ a | yes | 0.005 |
| 15,390.66 | | pP 44a | 15,390.65849 | 0.181 | pP 44a 4 0 1 1 0 0 E′ | yes | 0.002 |
| 15,390.514 | | unassigned | | | | | |
| 15,390.514 | | (pP 31s?) | 15,390.50993 | 0.047 | pP 31s 5 0 0 0 0 0 $A_1'$ s | yes | 0.004 |
| 15,383.381 | 2.97 | pP 43s | 15,383.37574 | 0.255 | pP 43s 4 0 1 1 0 0 E′ s | yes | 0.005 |
| 15,380.35 | 4.4 | pP 43a | 15,380.34811 | 0.155 | pP 43a 4 0 1 1 0 0 E′′ a | yes | 0.002 |
| 15,376.555 | 2.65 | pP 55a | 15,376.55023 | 0.177 | pP 55a 4 0 1 1 0 0 E′′ a | yes | 0.005 |
| 15,354.47 | 2.41 | pP 40a | 15,354.46842 | 0.177 | pP 40a 4 0 1 1 0 0 E′′ a | yes | 0.002 |

**Table 5**
Comparison of this work with the results of Coy and Lehmann [25] for the 18 000 $cm^{-1}$ region. Intensities, *I*, are absolute for Coy and Lehmann but are only relative (arbitrary units) for this work. $\Delta\tilde{\nu}$ is the wavenumber difference given as previous minus this work.

| Coy and Lehmann | | | This work | | | Agree? | $\Delta\tilde{\nu}/cm^{-1}$ |
|---|---|---|---|---|---|---|---|
| $\tilde{\nu}(cm^{-1})$ | $I(cm^{-1}$/km-atm) | assignment | $\tilde{\nu}(cm^{-1})$ | $I$ | assignment | | |
| 18,171.239 | 0.53 | qR 30 s | 18,171.23895 | 0.027 | qR 30s 5 0 1 1 0 0 E′′ a | yes | 0.000 |
| 18,154.944 | | rR 33 s | 18,154.95901 | 0.062 | | no | −0.015 |
| 18,154.869 | 1.6 | rR 33 a | 18,154.87596 | 0.026 | rR 22a 5 0 1 1 0 0 E′′ a | no | −0.007 |
| 18,153.669 | 0.3 | rR 33 s | 18,153.66587 | 0.022 | rR 33s 5 0 1 1 0 0 E′ s | yes | 0.003 |
| 18,143.119 | 0.53 | qR 10 s | 18,143.11963 | 0.027 | | no | −0.001 |
| 18,138.611 | 0.49 | rR 10 s | 18,138.61399 | 0.038 | rR 10s 5 0 1 1 0 0 E′ s | yes | −0.003 |
| 18,122.959 | 0.59 | rR 00 a | 18,122.95826 | 0.054 | rR 00a 5 0 1 1 0 0 E′′ a | yes | 0.001 |
| 18,105.057 | 0.46 | qQ 33 s | 18,105.05388 | 0.029 | pP 43a 5 0 1 1 0 0 E′′ a | no | 0.003 |
| 18,102.89 | | rQ 10 s | 18,102.89173 | 0.059 | rQ 10s 5 0 1 1 0 0 E′ s | yes | −0.002 |
| 18,102.70 | 0.89 | pQ 21 s | 18,102.70777 | 0.008 | qQ 22a 6 0 0 0 0 0 $A_1'$ s | no | −0.004 |
| 18,101.18 | 0.56 | | 18,101.18162 | 0.042 | | | −0.001 |
| 18,100.60 | | qQ 32 s | 18,100.59630 | 0.005 | | no | 0.001 |
| 18,100.49 | | | 18,100.49069 | 0.015 | qQ 33a 6 0 0 0 0 0 E′ s | | −0.006 |
| 18,100.4 | 0.52 | qQ 44 s | 18,100.40051 | 0.009 | | no | −0.001 |
| 18,099.62 | 0.82 | rQ 20 s | 18,099.61923 | 0.051 | rQ 31a 5 0 1 1 0 0 E′′ a | no | 0.001 |
| 18,089.05 | 1 | | 18,089.05126 | 0.060 | | | −0.001 |
| 18,075.534 | 0.46 | rQ 43 a | 18,075.53319 | 0.019 | | no | 0.001 |
| 18,062.524 | | pP 33 a | 18,062.52636 | 0.021 | | no | −0.002 |
| 18,062.524 | | rP 20 a | 18,062.52636 | 0.021 | qP 20a 6 0 0 0 0 0 E′ s | yes | −0.002 |
| 18,062.447 | 0.95 | pP 33 a | 18,062.44688 | 0.022 | | no | 0.000 |
| 18,010.338 | 0.42 | rP 40 a | 18,010.3395 | 0.030 | rP 40a 5 0 1 1 0 0 E′′ a | yes | −0.001 |

The majority of the remaining unassigned lines probably belong to states with higher rotational quantum numbers. The assignments were made using room-temperature ammonia line lists calculated with both an *ab initio* PES and a PES refined to experimental energy levels. An *ab initio* DMS has been used in the both line lists.

As the spectral region analysed in this work represents extrapolation to high energies from known ammonia spectra (the highest conventional FTS spectra of ammonia analysed as yet is in the 1 μm region [37]), quite large discrepancies between the observed and calculated energy levels are obtained. In particular, differences of 13 $cm^{-1}$ for the 15,000 $cm^{-1}$ region and about 25 $cm^{-1}$ for 18,000 $cm^{-1}$ region are found for our *ab initio* predictions. However this difference is largely due to use of a less well-converged basis set in the line list calculations. Significantly smaller discrepancies are observed for the better converged values of *ab initio* calculations presented previously [28].

Our assigned optical spectra of ammonia, which are given in the supplementary data, represent a significant expansion of the known spectral position of $NH_3$ lines. It provides a sound basis for the observation and analysis of the multiple resonance spectra of ammonia towards higher vibrational stretching states with $\nu_{NH}$ =7, 8 and higher up to dissociation. The way to this using two and three photon techniques has been demonstrated for water [38–40]. The highly excited stretching energy levels of water, derived from these papers, were used in the fit of the water PES to the experimental data. The resulting global water PES provided the means to compute the first complete water line list, which included every rovibrational bound state [41]. The present study of the optical spectrum of ammonia represents an important step towards the goal of calculating a complete line list for ammonia.

## Acknowledgement

This work was supported by the ERC Advanced Investigator Project 267219, the UK Natural Environment Research Council under grant NE/N001508/1. The State Project IAP RAS No. 0035-2014-009 is acknowledged by RIO, AAK, and NFZ. The National Solar Observatory is operated by the Association of Universities for Research in Astronomy, Inc., under contract with the National Science Foundation. Some support was provided by the NASA laboratory astrophysics program.

## Supplementary material

Supplementary material associated with this article can be found, in the online version, at doi:10.1016/j.jqsrt.2018.02.001.

## References

[1] Rothman LS, Gordon IE, Barbe A, Benner DC, Bernath PF, Birk M, Boudon V, Brown LR, Campargue A, Champion JP, Chance K, Coudert LH, Dana V, Devi VM, Fally S, Flaud JM, Gamache RR, Goldman A, Jacquemart D, Kleiner I, Lacome N, Lafferty WJ, Mandin JY, Massie ST, Mikhailenko SN, Miller CE, Moazzen-Ahmadi N, Naumenko OV, Nikitin AV, Orphal J, Perevalov VI, Perrin A, Predoi-Cross A, Rinsland CP, Rotger M, Simeckova M, Smith MAH, Sung K, Tashkun SA, Tennyson J, Toth RA, Vandaele AC, Auwera JV. The *HITRAN* 2008 molecular spectroscopic database. J Quant Spectrosc Radiat Transf 2009;110:533–72.

[2] Lundsberg-Nielsen L, Hegelund F, Nicolaisen FM. Analysis of the high--resolution spectrum of ammonia ($^{14}NH_3$) in the near-infrared region, 6400–6900 $cm^{-1}$. J Mol Spectrosc 1993;162:230–45.

[3] Li L, Lees RM, Xu LH. External cavity tunable diode laser spectra of the $\nu_1 + 2\nu_4$ stretch-band combination bands of $^{14}NH_3$ and $^{15}NH_3$. J Mol Spectrosc 2007;243:219–26.

[4] Lees RM, Li L, Xu LH. New VISTA on ammonia in the 1.5 $\mu$m region: assignments for the $\nu_3 + 2\nu_4$ bands of $^{14}NH_3$ and $^{15}NH_3$ by isotopic shift labeling. J Mol Spectrosc 2008;251:241–51.

[5] Sung K, Brown LR, Huang X, Schwenke DW, Lee TJ, Coy SL, Lehmann KK. Extended line positions, intensities, empirical lower state energies and quantum assignments of $NH_3$ from 6300 to 7000 $cm^{-1}$. J Quant Spectrosc Radiat Transfer 2012;113:1066–83. doi:10.1016/j.jqsrt.2012.02.037.

[6] Földes T, Golebiowski D, Herman M, Softley TP, Di Lonardo G, Fusina L. Low-temperature high-resolution absorption spectrum of $^{14}NH_3$ in the $\nu_1 + \nu_3$ band region (1.51 μm). Mol Phys 2014;112:2407–18.

[7] Barton EJ, Yurchenko SN, Tennyson J, Béguier S, Campargue A. A near infrared line list for $NH_3$: analysis of a kitt peak spectrum after 35 years. J Mol Spectrosc 2016;325:7–12. doi:10.1016/j.jms.2016.05.001.

[8] Barton EJ, Yurchenko SN, Tennyson J, Clausen S, Fateev A. High-resolution absorption measurements of $NH_3$ at high temperatures: 2100 - 5500 $cm^{-1}$. J Quant Spectrosc Radiat Transf 2017;189:60–5. doi:10.1016/j.jqsrt.2016.11.009.

[9] Gordon IE, Rothman LS, Hill C, Kochanov RV, Tan Y, Bernath PF, Birk M, Boudon V, Campargue A, Chance KV, Drouin BJ, Flaud JM, Gamache RR, Hodges JT, Jacquemart D, Perevalov VI, Perrin A, Shine KP, Smith MAH, Tennyson J, Toon GC, Tran H, Tyuterev VG, Barbe A, Császár AG, Devi VM, Furtenbacher T, Harrison JJ, Hartmann JM, Jolly A, Johnson TJ, Karman T, Kleiner I, Kyuberis AA, Loos J, Lyulin OM, Massie ST, Mikhailenko SN, Moazzen-Ahmadi N, Müller HSP, Naumenko OV, Nikitin AV, Polyansky OL, Rey M, Rotger M, Sharpe SW, Sung K, Starikova E, Tashkun SA, Vander Auwera J, Wagner G, Wilzewski J, Wcisło P, Yu S, Zak EJ. The HITRAN 2016 molecular spectroscopic database. J Quant Spectrosc Radiat Transf 2017;203:3–69. doi:10.1016/j.jqsrt.2017.06.038.

[10] Al Derzi AR, Furtenbacher T, Yurchenko SN, Tennyson J, Császár AG. MARVEL analysis of the measured high-resolution spectra of $^{14}NH_3$. J Quant Spectrosc Radiat Transf 2015;161:117–30. doi:10.1016/j.jqsrt.2015.03.034.

[11] Canty JI, Lucas PW, Tennyson J, Yurchenko SN, Leggett SK, Tinney CG, Jones HRA, Burningham B, Pinfield DJ, Smart RL. Methane and ammonia in the near-infrared spectra of late T dwarfs. Mon Not R Astron Soc 2015;450:454–80. doi:10.1093/mnras/stv586.

[12] Lucas PW, Tinney CG, Burningham B, Leggett SK, Pinfield DJ, Smart R, Jones HRA, Marocco F, Barber RJ, Yurchenko SN, Tennyson J, Ishii M, Tamura M, Day-Jones AC, Adamson A, Allard F, Homeier D. The discovery of a very cool, very nearby brown dwarf in the galactic plane. Mon Not R Astron Soc 2010;408:L56–60.

[13] Schneider AC, Cushing MC, Kirkpatrick JD, Gelino CR, Mace GN, Wright EL, Eisenhardt PR, Skrutskie MF, Griffith RL, Marsh KA. Hubble space telescope spectroscopy of brown dwarfs discovered with the wide-field infrared survey explorer. Astrophys J 2015;804:92. doi:10.1088/0004-637X/804/2/92.

[14] Tinetti G, Vidal-Madjar A, Liang MC, Beaulieu JP, Yung Y, Carey S, Barber RJ, Tennyson J, Ribas I, Allard N, Ballester GE, Sing DK, Selsis F. Water vapour in the atmosphere of a transiting extrasolar planet. Nature 2007;448:169–71.

[15] Moses JI, Visscher C, Fortney JJ, Showman AP, Lewis NK, Griffith CA, Klippenstein SJ, Shabram M, Friedson AJ, Marley MS, Freedman RS. Disequilibrium carbon, oxygen, and nitrogen chemistry in the atmospheres of HD 189733b and HD 209458b. Astrophys J 2011;737:15. doi:10.1088/0004-637X/737/1/15.

[16] Beaulieu JP, Tinetti G, Kipping D, Ribas I, Barber RJ, Cho JYK, Polichtchouk I, Tennysson J, Yurchenko SN, Griffith CA, Waldmann I, Miller S, Carey S, Mousis O, Fossey SJ, Aylward A. Methane in the atmosphere of the transiting hot neptune GJ436b? Astrophys J 2011;731:16.

[17] Seager S, Bains W, Hu R. Biosignature gases in $H_2$-dominated atmospheres on rocky exoplanets. Astrophys J 2013;777:95.

[18] Bains W, Seager S, Zsom A. Photosynthesis in hydrogen-dominated atmospheres. Life 2014;4:716–44. doi:10.3390/life4040716.

[19] MacDonald RJ, Madhusudhan N. HD 209458b in new light: evidence of nitrogen chemistry, patchy clouds and sub-solar water. Mon Not R Astron Soc 2017;469:1979–96. doi:10.1093/mnras/stx804.

[20] Csaszar AG, Furtenbacher T. Promoting and inhibiting tunneling via nuclear motions. Phys Chem Chem Phys 2016;18:1092–104. doi:10.1039/c5cp04270d.

[21] Huang X, Schwenke DW, Lee TJ. Rovibrational spectra of ammonia. II. Detailed analysis, comparison, and prediction of spectroscopic assignments for $^{14}NH_3$, $^{15}NH_3$, and $^{14}ND_3$. J Chem Phys 2011;134:044321.

[22] Boyarkin OV, Koshelev MA, Aseev O, Maksyutenko P, Rizzo TR, Zobov NF, Lodi L, Tennyson J, Polyansky OL. Accurate bond dissociation energy of water determined by triple-resonance vibrational spectroscopy and ab initio calculations. Chem Phys Lett 2013;568–569:14–20.

[23] Grechko M, Maksyutenko P, Rizzo TR, Boyarkin OV. Communication: Feshbach resonances in the water molecule revealed by state-selective spectroscopy. J Chem Phys 2010;133:081103.

[24] Kuga T, Shimizu T, Ueda Y. Observation and analysis of visible overtone band transitions of $NH_3$. Jap J Appl Phys 1985;24:L147.

[25] Coy SL, Lehmann KK. Rotational structure of ammonia NH stretch overtones: five and six quanta bands. J Chem Phys 1986;84:5239–49.

[26] Lehmann KK, Coy SL. Spectroscopy and intramolecular dynamics of highly excited vibrational states of $NH_3$. J Chem Soc Faraday Trans II 1988;84:1389–406.

[27] Coy SL, Lehmann KK. Modeling the rotational and vibrational structure of the i.r. optical spectrum of $NH_3$. Spectrochim Acta 1989;45A:47–56.

[28] Polyansky OL, Ovsyannikov RI, Kyuberis AA, Lodi L, Tennyson J, Yachmenev A, Yurchenko SN, Zobov NF. Calculation of rotation-vibration energy levels of the ammonia molecule based on an *ab initio* potential energy surface. J Mol Spectrosc 2016;327:21–30. doi:10.1016/j.jms.2016.08.003.

[29] Rothman LS, Gordon IE, Babikov Y, Barbe A, Benner DC, Bernath PF, Birk M, Bizzocchi L, Boudon V, Brown LR, Campargue A, Chance K, Cohen EA, Coudert LH, Devi VM, Drouin BJ, Fayt A, Flaud JM, Gamache RR, Harrison JJ, Hartmann JM, Hill C, Hodges JT, Jacquemart D, Jolly A, Lamouroux J, Le Roy RJ, Li G, Long DA, Lyulin OM, Mackie CJ, Massie ST, Mikhailenko S, Müller HSP, Naumenko OV, Nikitin AV, Orphal J, Perevalov V, Perrin A, Polovtseva ER, Richard C, Smith MAH, Starikova E, Sung K, Tashkun S, Tennyson J, Toon GC, Tyuterev VG, Wagner G. The *HITRAN* 2012 molecular spectroscopic database. J Quant Spectrosc Radiat Transf 2013;130:4–50. doi:10.1016/jqsrt.2013.07.002.

[30] Coles PA, Yurchenko SN, Polyansky OL, Kyuberis AA, Ovsyannikov RI, Zobov NF, Tennyson J. High accuracy potential energy surface, rovibrational energies and line list calculations for ammonia. *J Mol Spectrosc*, (To be submitted).
[31] Ovsyannikov RI, Coles PA, Yurchenko SN, Polyansky OL, Kyuberis AA, Zobov NF, Tennyson J. High accuracy potential and dipole moment surfaces for ammonia. *J Mol Spectrosc*, (To be submitted).
[32] Yurchenko SN, Thiel W, Jensen P. Theoretical ROVibrational Energies (TROVE): a robust numerical approach to the calculation of rovibrational energies for polyatomic molecules. J Mol Spectrosc 2007;245:126–40. doi:10.1016/j.jms.2007.07.009.
[33] Tennyson J, Yurchenko SN. The ExoMol project: software for computing molecular line lists. Intern J Quantum Chem 2017;117:92–103. doi:10.1002/qua.25190.
[34] Yurchenko SN, Barber RJ, Tennyson J. A variationally computed hot line list for $NH_3$. Mon Not R Astron Soc 2011;413:1828–34. doi:10.1111/j.1365-2966.2011.18261.x.
[35] Tennyson J, Yurchenko SN. ExoMol: molecular line lists for exoplanet and other atmospheres. Mon Not R Astron Soc 2012;425:21–33. doi:10.1111/j.1365-2966.2012.21440.x.
[36] Polyansky OL, Zobov NF, Viti S, Tennyson J, Bernath PF, Wallace L. K band spectrum of water in sunspots. Astrophys J 1997;489:L205–8.
[37] Barton EJ, Polyansky OL, Yurchenko SN, Tennyson J, Civis S, Ferus M, Hargreaves R, Ovsyannikov I, Kyuberis AA, Zobov NF, Béguier S, Campargue A. Absorption spectra of ammonia near 1 µm. J Quant Spectrosc Radiat Transf 2017;203:392–7. doi:10.1016/j.jqsrt.2017.03.042.
[38] Grechko M, Boyarkin OV, Rizzo TR, Maksyutenko P, Zobov NF, Shirin S, Lodi L, Tennyson J, Császár AG, Polyansky OL. State-selective spectroscopy of water up to its first dissociation limit. J Chem Phys 2009;131:221105.
[39] Maksyutenko P, Muenter JS, Zobov NF, Shirin SV, Polyansky OL, Rizzo TR, Boyarkin OV. Approaching the full set of energy levels of water. J Chem Phys 2007;126:241101.
[40] Grechko M, Maksyutenko P, Zobov NF, Shirin SV, Polyansky OL, Rizzo TR, Boyarkin OV. Collisionally assisted spectroscopy of water from 27 000 to 34 000 $cm^{-1}$. J Phys Chem A 2008;112:10539–45.
[41] Polyansky OL, Kyuberis AA, Lodi L, Tennyson J, Ovsyannikov RI, Zobov N, Yurchenko SN. Exomol molecular line lists XXVII: a complete high-accuracy line list for water. *Mon Not R Astron Soc*; In preparation.